Int. J. Electrochem. Sci., 7 **(2012)** 2504 - 2512

International Journal of
ELECTROCHEMICAL
SCIENCE
www.electrochemsci.org

Synthesis of Spinel $LiNi_xMn_{2-x}O_4$ (x=0, 0.1, 0.16) and Their High Rate Charge-Discharge Performances

Xin Gu, Xiaowei Li, Liqiang Xu, Huayun Xu[*]*, Jian Yang*[*]*, Yitai Qian*

Key Laboratory of Colloid and Interface Chemistry (Shandong University), Ministry of Education, and School of Chemistry and Chemical Engineering, Shandong University, Jinan 250100, P.R. China
[*]E-mail: xuhuayun@sdu.edu.cn; yangjian@sdu.edu.cn

Received: 11 January 2012 / *Accepted:* 8 February 2012 / *Published:* 1 March 2012

$LiNi_xMn_{2-x}O_4$ (x=0, 0.1, 0.16) were synthesized at 800 ℃ by a solid-state reaction from $LiNO_3$, $Ni(CH_3COO)_2$ and β-MnO_2. The XRD pattern confirmed the spinel structure of $LiNi_xMn_{2-x}O_4$ samples without any impurities. As the Ni content increased, the shape of the $LiNi_xMn_{2-x}O_4$ samples transformed from nanorods at x = 0 to truncated octahedrons at x = 0.1, 0.16, indicating the great effect of the doping on crystal growth. Among the three samples, $LiNi_{0.1}Mn_{1.9}O_4$ exhibits the best electrochemical performance, with 90% of capacity retention at a rate of 1 C, 90 % for 2 C and 92 % for 5 C after 1000 cycles at 25 ℃. Both XRD and CV results after 1000 cycles at a rate of 5 C revealed that Ni-doping could effectively preserve the structure of $LiMn_2O_4$ during the charge/discharge process. Even at 55 ℃, 80% of the discharge capacity was maintained at a rate of 5 C after 300 cycles.

Keywords: Inorganic compounds, Chemical synthesis, Electrochemical properties.

1. INTRODUCTION

$LiMn_2O_4$ spinel as one of the most promising cathode materials attracts extensive attention, due to its low cost, environmental friendliness and good safety [1]. However, the $LiMn_2O_4$-based cathode for lithium ion batteries suffers severe capacity loss especially at elevated temperature, which might be related with Mn dissolution in acidic electrolytes [2], Jahn-Teller distortion of Mn^{3+} at deeply discharge state [3], and oxygen deficiency [4]. In order to address the issues, using the other transitional metal (e.g. Ni, Fe, Co, Al) to replace Mn have been explored for the cathodes of lithium ion batteries [5-8]. Among these materials, $LiNi_xMn_{2-x}O_4$ shows the best cycling stability, triggering the intensive studies in this field [9, 10]. This improvement probably comes from the strong chemical bond of Mn-O-Ni that stabilizes the octahedral spinel sites, prevents the dissolution of Mn^{3+} ions into the electrolyte, and restrains the Jahn-Teller distortion [11]. Since a large amount of Ni doping could

render a significant decrease of the capacity at 4 V [12], most studies about $LiNi_xMn_{2-x}O_4$ were confined in the case of $x \leq 0.2$ for stable crystal structure and good cyclic performance [13-16]. So far, the performance of $LiNi_xMn_{2-x}O_4$ at room temperature has been well documented, but that at elevated temperature is studied to a less extent [17,18], particularly at a high-rate charge/discharge. It was reported that $Li_{1.06}Ni_{0.01}Mn_{1.93}O_4$ displayed a capacity retention value of 90.4% at a rate of 1 C after 100 cycles at 55 ℃ [17]. $Li_{1.05}Ni_{0.05}Mn_{1.9}O_4$ kept 85% of the capacity at a rate of 1 C after 100 cycles at 55 °C [18]. The lower current density and the less cycling number in these reports cannot completely reflect the performance of $LiNi_xMn_{2-x}O_4$ as a cathode at elevated temperature.

The electrochemical property of $LiMn_2O_4$-based spinel highly depends on its synthetic routes, such as the Pechini process [19], sol-gel [20], emulsion method [21], the citric method [22], etc. However, most of these methods involve complicate treatment processes or expensive reagent, which is time consuming and high cost for commercial applications. In this work, $LiNi_xMn_{2-x}O_4$ (x=0, 0.1, 0.16) spinels were synthesized at 800 ℃ from $LiNO_3$, $Ni(CH_3COO)_2$ and β-MnO_2. XRD patterns of $LiNi_xMn_{2-x}O_4$ samples can be indexed to a spinel structure. SEM images show that the morphologies of $LiNi_xMn_{2-x}O_4$ are nanorods as x=0 and truncated octahedrons as x=0.1, 0.16. Among these samples, $LiNi_{0.1}Mn_{1.9}O_4$ exhibits enhanced rate capability and high rate cycling performances both at room temperature and 55 ℃. The structure stability was confirmed by XRD and CV measurements after long-term cycling.

2. EXPERIMENTAL

The synthetic route of $LiNi_xMn_{2-x}O_4$ (x=0, 0.1, 0.16) was as follows: lithium nitrate, nickel acetate and β-MnO_2 nanowires with a molar ratio of 1.02: x: (2-x) were dispersed in 100 mL of deionized water. After a homogeneous mixture was produced, water was gradually evaporated at 100 ℃ under constantly stirring. The obtained powder was then annealed at 800 ℃ for 12 h and cooled to room temperature naturally. β-MnO_2 nanowires were hydrothermally prepared at 150 ℃ for 12 h according to the literature [23].

X-ray diffraction was carried out by an advanced X-ray diffractometer of Bruker D8 based on Ni-filtered Cu Kα-radiation (λ=1.5418 Å). XRD data were obtained at 2θ of 10°~70°. The morphologies of the samples were observed by a field emission scanning electron microscope (FESEM, JEOL JSM-6700F).

The composite electrodes for electrochemical studies were prepared with active material, conductive carbon black and poly(vinylidene fluoride) (PVDF) in the ratio of 80:10:10 (in wt%). N-methyl-2-pyrrolidone (NMP) was used as the solvent. The slurry was coated on an aluminum foil, dried at 120 ℃ for 12 h and finally rolled. The typical cathode loading was 3~4 mg/cm^2 and the active material was around 2~4 mg. The coin cells of type CR2032 were assembled in an argon-filled glove box with lithium metal foil as the counter and the reference electrode. A 1 M solution of $LiPF_6$ in ethylene carbonate (EC), diethyl carbonate (DEC), dimethyl carbonate (DMC) (1:1:1, by volume) was used as the electrolyte with a Celgard 2400 microporous polypropylene membrane as the separator. Cyclic voltammetry experiments were carried out between 3.4~4.4 V at a scan rate of 0.1 mV s^{-1} using

a LK2005A Electrochemical Workstation. Galvanostatic charge-discharge tests were performed using a LAND CT2001A system. The charge-discharge cycles were studied at different current rates (1 C = 150 mA/g) between 3.4~4.4 V at 25 ℃ and 55 ℃.

3. RESULTS AND DISCUSSION

3.1. Structure and morphology characterization

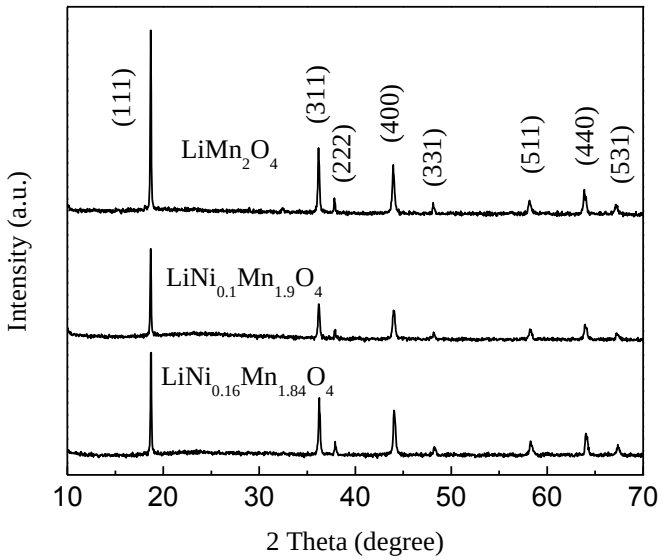

Figure 1. X-ray diffraction patterns of $LiNi_xMn_{2-x}O_4$ (x=0, 0.1, 0.16) samples

Fig. 1 shows the XRD patterns of $LiNi_xMn_{2-x}O_4$ (x=0, 0.1, 0.16) prepared by high-temperature synthesis. All the peaks in these XRD patterns could be assigned to a spinel structure. No impurities like nickel oxides and MnO_x, are observed in the product. The calculated lattice constant of $LiNi_xMn_{2-x}O_4$ (x=0, 0.1, 0.16) is 8.229(5) Å, 8.221(6) Å and 8.214(0) Å, respectively. It is noted that the lattice constant slightly decreases with the increasing of the Ni content, which can be explained by the ionic size effect [24]. This lattice contraction also indicates the successful substitution of Ni for Mn in the product.

Fig. 2 shows the SEM images of β-MnO_2 nanowires and $LiNi_xMn_{2-x}O_4$ (x=0, 0.1, 0.16) prepared by high-temperature synthesis. The β-MnO_2 nanowires as the precursor in the reaction are in the diameter of 50-80 nm and tens of micrometers in length (Fig. 2a). After reacted at high temperature, the as-obtained $LiNi_xMn_{2-x}O_4$ (x=0, 0.1, 0.16) has significant changes in morphology. In the case of x = 0, $LiMn_2O_4$ displays a rod-like shape with the diameter of ~ 200 nm and length up to several micrometers, as shown in Fig. 2b. Compared with that of MnO_2 nanowires, the length of the $LiMn_2O_4$ nanorods is significantly shortened, which can be explained by the high-temperature induced shape contraction. The shapes of $LiNi_xMn_{2-x}O_4$ (x= 0.1, 0.16) particles are truncated octahedron, totally

different from the $LiMn_2O_4$ nanorods. This result indicates the great effect of doping on the shape of the product, which is also reported in the doping of other elements into $LiMn_2O_4$ [25].

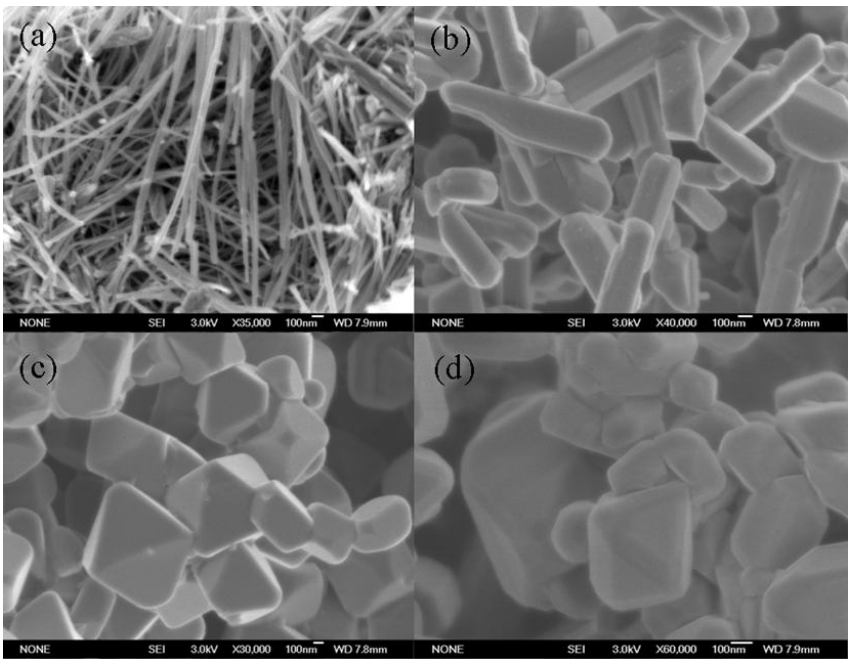

Figure 2. FESEM images of (a) β-MnO_2 precursor, (b) $LiMn_2O_4$, (c) $LiNi_{0.1}Mn_{1.9}O_4$, (d) $LiNi_{0.16}Mn_{1.84}O_4$ samples

3.2 Cyclic voltammetry studies

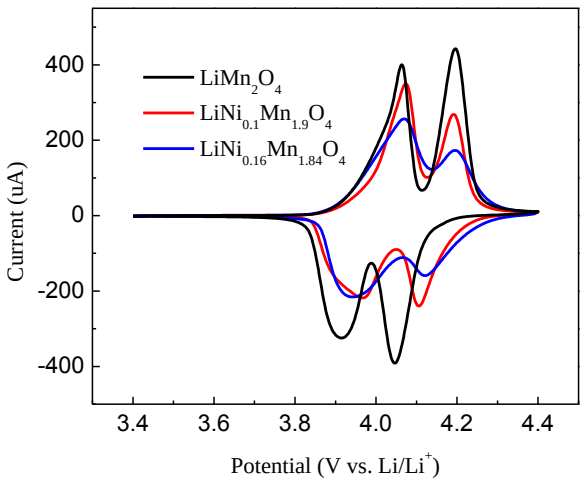

Figure 3. Cyclic voltammetry (CV) profiles of $Li/LiNi_xMn_{2-x}O_4$ (x=0, 0.1, 0.16) cells at a scan rate of 0.1 mV s^{-1}

Fig. 3 presents the cyclic voltammogram profiles of $Li/LiNi_xMn_{2-x}O_4$ (x=0, 0.1, 0.16) between 3.4 and 4.4 V at a scan rate of 0.1 mV s^{-1}. For $Li/LiMn_2O_4$, the CV curve shows two well-resolved

peaks around 4.19 V/4.06 V (oxidation peaks) and 4.04 V/3.91 V (reduction peaks), corresponding to the redox couple of Mn^{3+}/Mn^{4+} [26]. When the Ni ions are introduced into $LiMn_2O_4$, the peak areas gradually decrease with the increasing of the Ni content in the product. This result implies that only the Mn species makes the contribution to the charge-discharge capacities from 3.4 to 4.4 V. Meanwhile, the reduction peaks shift toward higher potential than that of pure $LiMn_2O_4$, indicating that the extraction of lithium ions becomes more and more difficult. The difference between the oxidation peak and the reduction one is reduced as the increase of Ni content in the product, indicating the decreased polarization of the electrodes.

3.3 Galvanostatic cycling studies

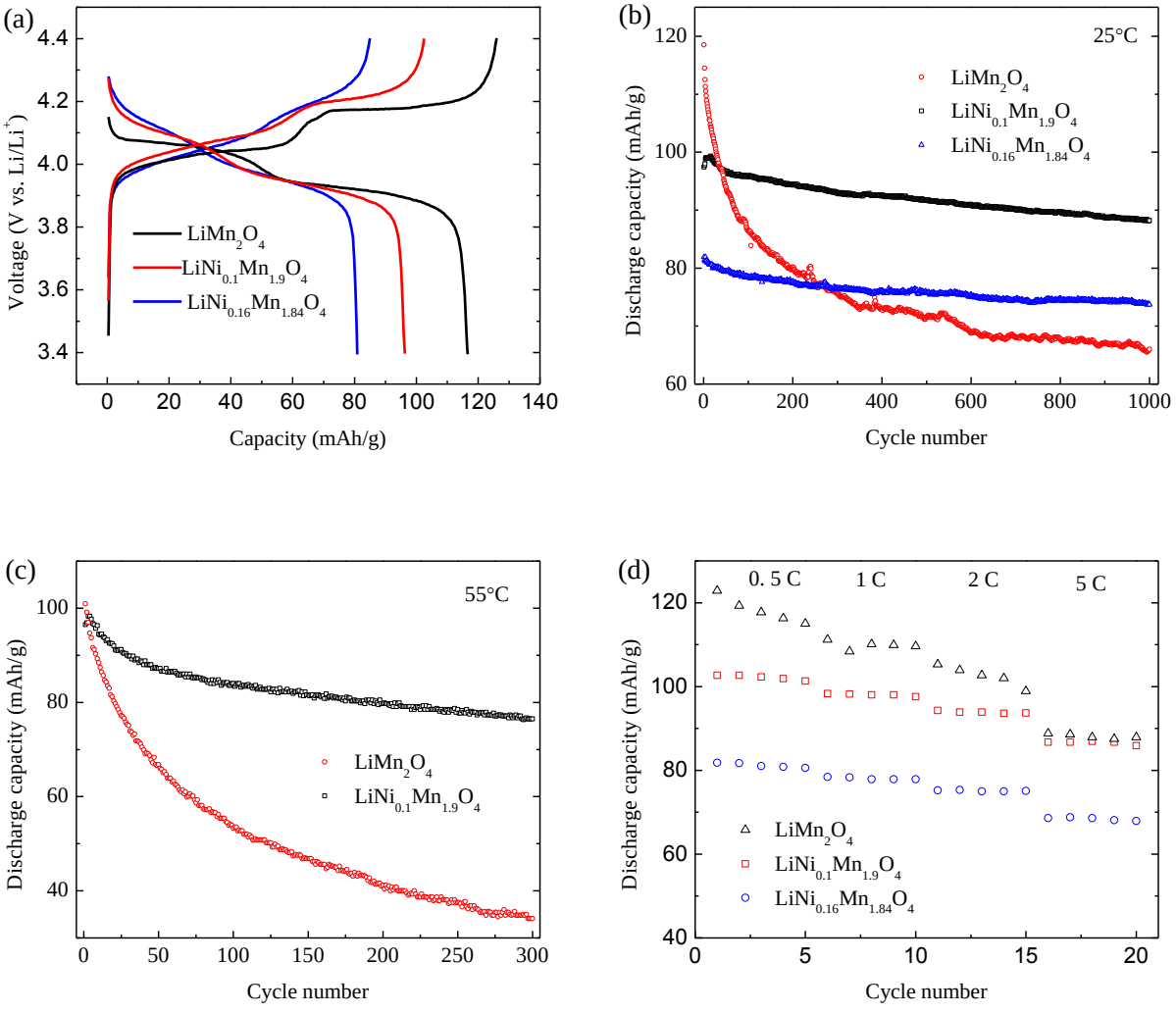

Figure 4. (a) Initial charge-discharge curves of $Li/LiNi_xMn_{2-x}O_4$ (x=0, 0.1, 0.16) cells in the voltage range of 3.4~4.4 V at 1 C rate;(b) Discharge capacity vs. cycle number of $Li/LiNi_xMn_{2-x}O_4$ (x=0, 0.1, 0.16) cells at 1 C rate at 25 ℃;(c) Discharge capacity vs. cycle number of $Li/LiMn_2O_4$ and $Li/LiNi_{0.1}Mn_{1.9}O_4$ cells at 5 C rate at 55 ℃;(d) Rate performance of the discharge capacity of $Li/LiNi_xMn_{2-x}O_4$ (x=0, 0.1, 0.16) cells at varied discharge rate from 0.5 to 5 C.

Fig. 4a shows the initial charge-discharge profiles of Li/$LiNi_xMn_{2-x}O_4$ (x=0, 0.1, 0.16) cells at 1 C rate between 3.4 and 4.4 V. The three electrodes exhibit two well-known plateau behaviors, corresponding to Li^+ extraction/insertion at different sites in the spinel framework [27, 28]. The charge voltage plateau of the Li/$LiNi_xMn_{2-x}O_4$ electrodes (x=0, 0.1, 0.16) is elevated gradually with increasing Ni-content, which is consistent with the cyclic voltammery result as shown in Fig. 3. The initial discharge capacity was about 118, 97, 82 mAh/g for the $LiNi_xMn_{2-x}O_4$ samples as x=0, 0.1, 0.16, respectively. The gradual decrease of reversible capacity for the first cycle was owing to the increasing Ni substitution for Mn.

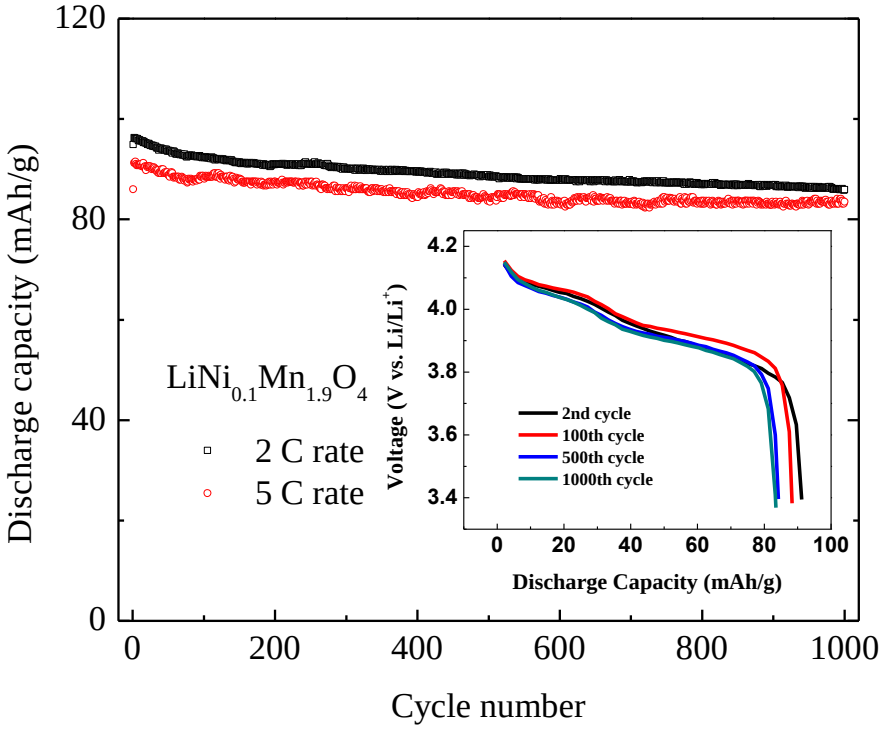

Figure 5. Long-term cycling performance of Li/$LiNi_{0.1}Mn_{1.9}O_4$ cells in the voltage range of 3.4~4.4 V cycled at 2 C and 5 C rates (Inset is the discharge profiles of Li/$LiNi_{0.1}Mn_{1.9}O_4$ cell along long-term charge-discharge processes at 5 C rate)

To evaluate the cycling stability, the discharge capacity of Li/$LiNi_xMn_{2-x}O_4$ electrodes (x=0, 0.1, 0.16) at a rate of 1 C up to 1000 cycles at 25 ℃ are shown in Fig. 4b. The capacity retention of $LiNi_xMn_{2-x}O_4$ samples at 25 ℃ are 56%, 90% and 90% for x=0, 0.1 and 0.16, respectively. The cycling performances of Li/$LiMn_2O_4$ and Li/$LiNi_{0.1}Mn_{1.9}O_4$ cells at 55 ℃ up to 300 cycles at a rate of 5C are shown in Fig. 4c. It shows that the capacity retention increases from 34% for pristine $LiMn_2O_4$ to 80% for the Ni-doping sample. That means the capacity loss per cycle for Li/ $LiNi_{0.1}Mn_{1.9}O_4$ cell is only 0.01% at 25 ℃ and 0.067% at 55 ℃. So, it is concluded that cycling stability of $LiMn_2O_4$ spinel is significantly improved by Ni-doping.

Fig. 4d shows the rate capability of $LiNi_xMn_{2-x}O_4$ samples (x=0, 0.1, 0.16) in the range of 3.4~4.4 V (5 cycles were carried out at each rate). The rate capability is expressed as the capacity at a

given discharge rate relative to that obtained at the rate of 0.5 C (75 mA/g). As x=0.1 and 0.16, the specific capacity retention at 5 C (750 mA/g) is 85% and 84% compared to that at 0.5 C, whereas only 76% retention is obtained when x=0. Therefore, we conclude that Ni doping can significantly improve the rate capability of $LiMn_2O_4$ spinel.

Fig. 5 shows the long-term cycling performance of $LiNi_{0.1}Mn_{1.9}O_4$ at the rate of 2 C and 5 C rate (the discharge profiles of Li/ $LiNi_{0.1}Mn_{1.9}O_4$ cell at 5 C rate is given in the inset of Fig. 5). At a rate of 2 C, Li/$LiNi_{0.1}Mn_{1.9}O_4$ cell shows a discharge capacity of 96 mAh/g and a capacity retention of 90% after 1000 cycles. At a rate of 5 C, Li/$LiNi_{0.1}Mn_{1.9}O_4$ displays a discharge capacity of 91 mAh/g and a capacity retention of 92% after 1000 cycles. Compared with the previous works in Table 1, our work displays a fair capacity at room temperature and at elevated temperature.

Table 1. Comparison of the capacity of this work and previous results at different charge rates

Sample	Capacity of 1st or 2nd cycle (m Ah/g)	Current density	Potential window (V)	Cycle number	Capacity retention (%)	Temperature (℃)	Reference
$LiNi_{0.04}Mn_{1.96}O_4$	84	0.5C	3.2-4.35	100	95	RT	[15]
$LiNi_{0.05}Mn_{1.95}O_4$	105	0.5C	3.1-4.4	100	90	25	[18]
$LiNi_{0.1}Mn_{1.9}O_4$	95	5C	3.5-4.4	—	—	RT	[16]
$Li_{1.05}Ni_{0.05}Mn_{1.9}O_4$	105	140mA/g	3.0-4.3	100	85	55	[13]
$LiNi_{0.1}Mn_{1.9}O_4$	92.4	0.2mA/cm^2	3.5-4.3	50	61.4	25	[5]
$LiNi_{0.1}Mn_{1.9}O_4$	80.3	0.2mA/cm^2	3.5-4.3	50	61.4	50	[5]
$Li_{1.06}Ni_{0.01}Mn_{1.93}O_4$	105.1	1C	3.2-4.4	100	96.4	25	[12]
$Li_{1.06}Ni_{0.01}Mn_{1.93}O_4$	105.7	1C	3.2-4.4	100	90.4	55	[12]
$LiNi_{0.1}Mn_{1.9}O_4$	97	1C	3.4-4.4	1000	90	25	This work
$LiNi_{0.1}Mn_{1.9}O_4$	96.5	5C	3.4-4.4	300	80	55	This work
$LiNi_{0.1}Mn_{1.9}O_4$	91	5C	3.4-4.4	1000	92	25	This work

3.4 Structure stability studies

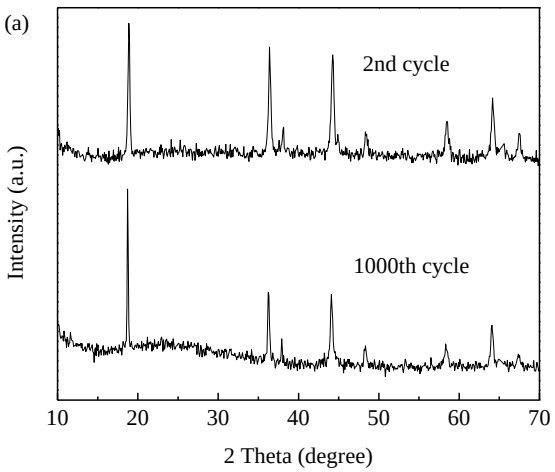

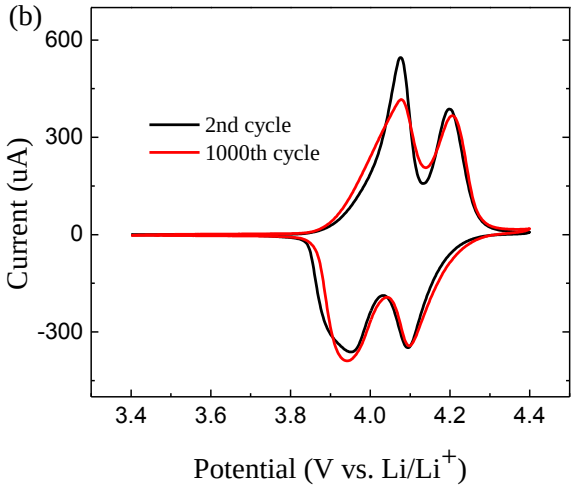

Figure 6 a) X-ray diffraction patterns of $LiNi_{0.1}Mn_{1.9}O_4$ composite electrodes after 2 and 1000 cycles at 5 C rate b) Cyclic voltammetry curves of $Li/LiNi_{0.1}Mn_{1.9}O_4$ cell after 2 and 1000 cycles at 5 C rate

X-ray diffraction is applied to investigate the structure of $LiNi_{0.1}Mn_{1.9}O_4$ after 2 and 1000 cycles. As given in Fig. 6a, it is found that no peak emerges or disappears after 1000 cycles compared to the second cycle, which indicates that the structure of $LiNi_{0.1}Mn_{1.9}O_4$ is almost unchanged after 1000 charge-discharge tests. The cyclic voltammetry test of $Li/LiNi_{0.1}Mn_{1.9}O_4$ cells after 1000 cycles is also carried out. As shown in Fig. 6b, the peak potentials keep almost unchanged and the peak currents only reduce slightly even after long-term cycle tests. Hence, both XRD and CV data confirm very well with the high rate charge-discharge performances and reveal that the structure of $LiMn_2O_4$ is stabilized by Ni-doping leading to improved electrochemical performances.

4. CONCLUSIONS

In conclusion, $LiNi_xMn_{2-x}O_4$ (x=0, 0.1, 0.16) were prepared by a solid state reaction starting from $LiNO_3$, $Ni(CH_3COO)_2$ and β-MnO_2 nanowires. Among these samples, $LiNi_{0.1}Mn_{1.9}O_4$ spinel exhibits enhanced electrochemical performances, with 90% capacity retention after 1000 cycles at 1 C rate at 25 ℃, and 80% after 300 cycles at 5 C rate at 55 ℃. Capacity retention values of 90% for 2 C rate and 92% for 5 C rate after 1000 cycles are obtained. The excellent cycling performance of $LiNi_{0.1}Mn_{1.9}O_4$ sample at high rate can be attributed to the structure stability which has been confirmed by both XRD and CV research after high rate long-term cycling.

ACKNOWLEDGEMENTS
This study was supported by the 973 Project of China (No.2011CB935901), the National Natural Science Foundation of China (Grant No. 20871075, No. 91022033), the Independent Innovation Foundations of Shandong University (2009TS017, 2009JC019) and new-faculty start-up funding in Shandong University. We are also grateful to the Graduate Independent Innovation Foundation of Shandong University (yzc11034).

References

1. T. Ohzuku, M. Kitagawa and T. Hirai, *J. Electrochem. Soc.*, 137 (1990) 769
2. D. Aurbach, M.D. Levi, K. Gamulski, B. Markovsky, G. Salitra, E. Levi, U. Heider, L. Heider and R. Oesten, *J. Power Sources*, 81 (1999) 472
3. M. Tabuchi, C. Masquelier, H. Kobayashi, R. Kanno, Y. Kobayashi, T. Akai, Y. Maki, H. Kageyama and O. Nakamura, *J. Power Sources*, 68 (1997) 623
4. Y.Y. Xia, T. Sakai, T. Fujieda, X.Q. Yang, Z.F. Ma, J. McBreen and M. Yoshio, *J. Electrochem. Soc.*, 148 (2001) A723
5. Y. Ito, Y. Idemoto, Y. Tsunoda and N. Koura, *J. Power Sources*, 119–121 (2003) 733
6. Q.H. Wu, J.M. Xu, Q.C. Zhuang and S.G. Sun, *Solid State Ionics*, 177 (2006) 1483
7. A. Sakunthala, M.V. Reddy, S. Selvasekarapandian, B.V.R. Chowdari and P.C. Selvin, *Electrochim. Acta*, 55 (2010) 4441
8. L.F. Xiao, Y.Q. Zhao, Y.Y. Yang, Y.L. Cao, X.P. Ai and H.X. Yang, *Electrochim. Acta*, 54 (2008) 545
9. Q. Zhong, A. Bonakdarpour, M. Zhang, Y. Gao and J.R. Dahn, *J. Electrochem. Soc.*, 144 (1997) 205
10. K. Amine, H. Tukamoto, H. Yasuda and Y. Fujita, *J. Power Sources*, 68 (1997) 604.
11. J. Shu, T.F. Yi, M. Shui, Y. Wang, R.S. Zhu, X.F. Chu, F.T. Huang, D. Xu and L. Hou, *Comput. Mat. Sci.*, 50 (2010) 776
12. R. Santhanam, B. Rambabu, *J. Power Sources*, 195 (2010) 5442
13. H.M. Wu, J.P. Tu, X.T. Chen, Y. Li, X.B. Zhao and G.S. Cao, *J. Solid State Electrochem.*, 11(2007) 173
14. L.Q. Zhang, T. Yabu and I. Taniguchi, *Mater. Res. Bull.*, 44 (2009) 707
15. I. Taniguchi, D. Song and M. Wakihara, *J. Power Sources*, 109 (2002) 333
16. J.M. Amarilla, R.M. Rojas, F. Pico, L. Pascual, K. Petrov, D. Kovacheva, M.G. Lazarraga, I. Lejona and J.M. Rojo, *J. Power Sources*, 174 (2007) 1212
17. J.M. Amarilla, K. Petrov, F. Pico, G. Avdeev, J.M. Rojo and R.M. Rojas, *J. Power Sources*, 191 (2009) 591
18. K.S. Lee, S.T. Myung, H.J. Bang, S. Chung and Y.K. Sun, *Electrochim. Acta*, 52 (2007) 5201
19. S.H. Wu, H.L. Chen, *J. Power Sources*, 119 (2003)134
20. X.M. Liu, Z.D. Huang, S. Oh, P.C. Ma, P.C.H. Chan, G.K. Vedam, K. Kang and J.K. Kim, *J. Power Sources*, 195 (2010) 4290
21. B.H. Kim, Y.K. Choi and Y.H. Choa, *Solid State Ionics*, 158 (2003) 281
22. W.S. Yang, Q.G. Liu, W.H. Qiu, S.G. Lu and L.L. Yang, *Solid State Ionics*, 121 (1999) 79
23. 23.X. Wang, Y.D. Li, *Chem-Eur. J.*, 9 (2003) 300
24. S. Mandal, R.M. Rojas, J.M. Amarilla, P. Calle, N.V. Kosova, V.F. Anufrienko and J.M. Rojo, *Chem. Mater.*, 14 (2002) 1598
25. S. Priti, S. Anjan, N. Mala and R. Subrata, *Physica B*, 405 (2010) 649
26. K.M. Shaju, G.V.S. Rao and B.V.R. Chowdari, *Solid State Ionics*, 148 (2002) 343
27. Y.J. Wei, K.B. Kim and G. Chen, *Electrochim. Acta*, 51 (2006) 3365
28. M.V. Reddy, S.S. Manoharan, J. John, B. Singh, G.V.S. Rao and B.V.R. Chowdari, *J. Electrochem. Soc.*, 156 (2009) A652